

Ανασκόπηση του Μονοδιάστατου Προτύπου Heisenberg και της Θεωρίας Επανακανονικοποίησης Ισχυρής Αταξίας

Βασίλειος Βαλατσός

Επιβλέπον Καθηγητής – Άρης Μουστάκας



Εθνικό και Καποδιστριακό Πανεπιστήμιο Αθηνών
Τμήμα Φυσικής
Τομέας Πυρηνικής Φυσικής και Στοιχειωδών Σωματιδίων
Αθήνα, 2021

Εισαγωγή

Η μέθοδος επανακανονικοποίησης ισχυρής αταξίας, όπως παρουσιάστηκε πρώτα από τους Dasgupta, Ma και Hu, δίνει ασύμπτωτικά ακριβή αποτελέσματα σε κατανομές όπου η αταξία αυξάνεται χωρίς όριο σε μεγάλες κλίμακες, ενώ αργότερα, ο Fisher, ο οποίος επέκτεινε την ιδέα, υπολόγισε και οριακές τιμές καθώς και συντελεστές κλίμακας για τυχαίες αλυσίδες σπιν.

Αυτά τα αποτελέσματα δεν ήταν παρά τα πρώτα πολλών που ακολούθησαν μέσω εντατικής έρευνας, πρώτα σε τυχαία κβαντικά συστήματα ενώ ύστερα προέκυψε και η επέκτασή τους σε κλασσικά άτακτα μοντέλα. Οι προηγούμενες μέθοδοι επανακανονικοποίησης αντιμετώπιζαν το σύστημα σε έναν ομογενή χώρο, το οποίο επέτρεπε την ομαδοποίηση των σπιν σε υπερσπιν και ενώ σε μη-τυχαία συστήματα αυτή η ομογένεια είναι φυσικά επιβεβαιώσιμη, τίθεται υπό ερώτημα παρουσία άτακτων συστημάτων. Η μέθοδος επανακανονικοποίησης ισχυρής αταξίας αντιθέτως, επανακανονικοποιεί τον χώρο με μη-ομογενή τρόπο, επιτρέποντας έτσι τον καλλίτερο χειρισμό τοπικών αταξιών.

Πιο συγκεκριμένα, η αλυσίδα XX, που πρώτα μελέτησε ο Fisher, δίνει ακριβή αποτελέσματα για την συμπεριφορά φάσεων στις οποίες κυριαρχεί η τυχειότητα, καθώς και για την κρίσιμη συμπεριφορά κοντά στις διάφορες αλλαγές φάσης που προκύπτουν σε μηδενική θερμοκρασία. Μελετώντας τις ιδιότητες της αντιφερρομαγνητικής αλυσίδας με σπιν- $\frac{1}{2}$ με τυχαίους δεσμούς, αναλύουμε της συμπεριφορά χαμηλής ενέργειας, σπώντας τον ισχυρότερο δεσμό και αντικαθιστώντας τον με έναν ενεργό δεσμό μεταξύ πλησιέστερων γειτόνων. Επαναλαμβάνοντας την διαδικασία, η κατανομή φαρδαίνει, βελτιώνοντας την ακρίβεια της προσέγγισης.

Η δομή της εργασίας είναι η εξής. Πρώτα εισαγάγουμε το πρότυπο Heisenberg και δείχνουμε την συσχέτισή του με τα πρότυπα του Ising και των ελευθέρων φερμιονίων, το λύνουμε ακριβώς στην φερρομαγνητική περίπτωση μέσω του άνσατς του Bethe, και εισαγάγουμε την μέθοδο επανακανονικοποίησης μέσω blocks για την αντιφερρομαγνητική περίπτωση. Στην συνέχεια παρουσιάζουμε την μέθοδο επανακανονικοποίησης ισχυρής αταξίας, χρησιμοποιώντας μια σύγχρονη μορφή της μεθόδου που ο Fisher χρησιμοποίησε για να λύσει την τυχαία αντιφερρομαγνητική XX αλυσίδα. Τέλος, παρουσιάζουμε τις μεθόδους που φτιάξαμε για να μοντελοποιήσουμε την διαδικασία με χρήση της προγραμματιστική γλώσσας Python.

Introduction

The SDRG method, first introduced by Dasgupta, Ma and Hu, and later greatly expanded by Fisher, yields asymptotically exact results in distributions where the disorder grows without limit in large scales, whilst Fisher also calculated limit values as well as scaling factors for random spin chains.

These results were the first of many, yielded through the intense research that followed afterwards, firstly in random quantum systems, and later expanded in classically disordered systems as well. The previous Real Space RG methods that were used treated the whole space as homogenous, allowing the grouping of spins into super-spins, and although in systems absent of randomness this homogeneity is physically verifiable, it comes into question in the presence of disordered systems. The SDRG method has the property of renormalising space in a non-homogenous way so it can better handle local disorders.

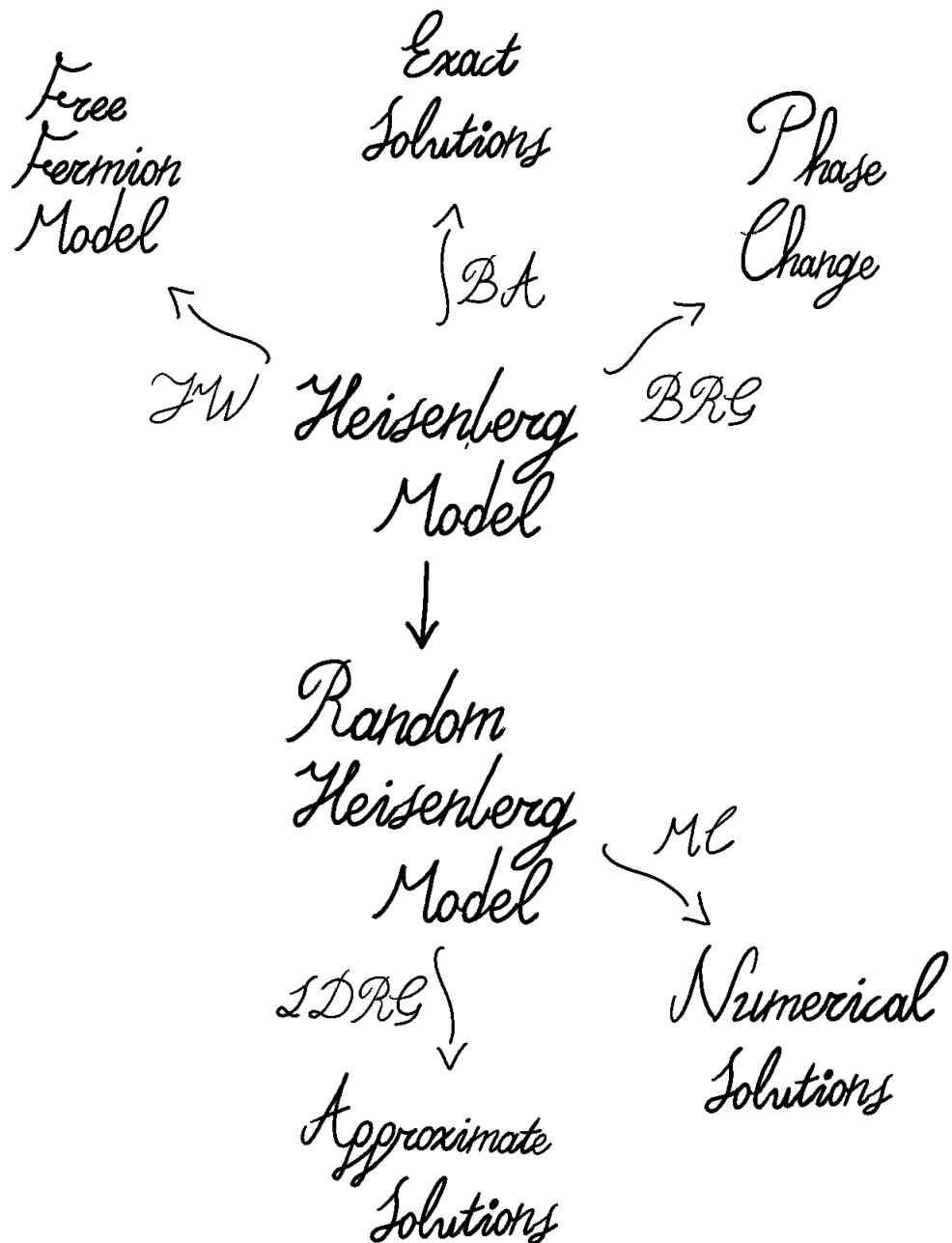
More specifically, the XX chain, presented by Fisher, can be used to obtain exact results for the behaviour of phases dominated by randomness, as well as the critical behaviour near the various zero temperature phase transitions that occur. Studying the properties of antiferromagnetic Heisenberg $\text{spin}^{-1/2}$ chains with random bonds, we analyse the low-energy behaviour, by decimating the strongest bond, replacing it with a new effective bond between the nearest neighbours. Repeating the procedure, the distribution becomes extremely broad improving the accuracy of the approximation.

The structure of the thesis is this. First we introduce the Heisenberg model, it's relation to the Ising and Free Fermion models, solve it exactly for the ferromagnetic case using the Bethe Ansatz and introduce the Block RG method for the antiferromagnetic case. Afterwards we present the Strong Disorder RG method, using a modernised version of Fisher's process to solve the random AF XX chain. Finally, we present the methods we created to simulate the process.

Contents

1	Introduction to the Heisenberg Model	1
1.1	Relation to the Ising Model	2
1.1.1	A Brief Discussion on Universality Classes	3
1.1.2	Ising and Heisenberg Universality Classes	3
1.2	Relation to the Free Fermion Model	4
2	Ferromagnetic Ground and Excited States	7
2.1	Excited States via the Bethe Ansatz	8
2.2	A Single Magnon	8
3	Real-Space Renormalisation Group	10
3.1	RSRG of the AF Heisenberg Model	10
3.1.1	Construction of the Effective Hamiltonian	12
3.1.2	Fixed Points	14
4	SDRG Method for the Random AF Model	15
4.1	Dasgupta-Ma RG Method for the Heisenberg Model	15
4.2	RG Flow Equation for the XX Chain	16
4.3	Fixed Points and the Random Singlet Phase	17
4.4	Physical Properties	19
4.4.1	Low Temperature Susceptibility	20
4.4.2	Average Pair Correlation Function	20
5	Numerical Dasgupta-Ma RG	22
5.1	Introduction to the Model	22
5.2	Results	25
	Appendices	27
A	The Heisenberg Hamiltonian	28
B	Perturbation of the Random XX Spin Chain	30
	Bibliography	32

Graphic Summary of the Thesis



1 | Introduction to the Heisenberg Model

A quantum spin chain consists of a one-dimensional lattice with N sites, where on each site we consider a spin particle, in the case of a $S=1/2$ particle an electron. This electron can either have spin up (denoted by $|\uparrow\rangle$) or down (denoted by $|\downarrow\rangle$) and, therefore, any electron exists in a linear state $a|\uparrow\rangle + b|\downarrow\rangle$, which generates a local two-dimensional Hilbert space. Since the lattice is of size N , we also have N electrons, so the total Hilbert space in which the states live is

$$H = \bigotimes_N \mathbb{C}^2 \quad (1.1)$$

The spin operators $S_i^{x,y,z}$ act on each site i and satisfy the local commutation relations

$$[S_i^a, S_j^b] = \delta_{ij} \epsilon^{abc} S_i^c, \quad i \neq j \quad (1.2)$$

The Hamiltonian describes a nearest neighbour interaction between the spins,

$$H = -J \sum_i \vec{S}_i \vec{S}_{i+1} \quad (1.3)$$

and we also demand that $\vec{S}_{N+1} = \vec{S}_1$.

If we expand the Hamiltonian writing the vector components, it is a special case of a more general Hamiltonian, with the form

$$H = - \sum_{i=1}^L (J^x S_i^x S_{i+1}^x + J^y S_i^y S_{i+1}^y + J^z S_i^z S_{i+1}^z) \quad (1.4)$$

Depending on the nature of J^x , J^y , J^z , one can find five different models, called

- The *XYZ – model*, where $J^x \neq J^y \neq J^z$
- The *XXZ – model*, where $J^x = J^y \neq J^z$
- The *XXX – model*, where $J^x = J^y = J^z$
- The *XY – model*, where $J^x \neq J^y$, and $J^z = 0$
- The *XX – model*, where $J^x = J^y$, and $J^z = 0$

Without loss of generality, we can assume that the signs of the J^x are the same for the whole chain, as well as for the y and z components individually. By rotating the spins around the z -axis, we can always assume that $J^x > 0$ and $J^y < 0$, so that the ferromagnetic nature of the model is characterised solely by the J^z . $J^z < 0$ means the antiferromagnetic, while $J^z > 0$ means the ferromagnetic model.

Another way to write the Hamiltonian, which will be of use for the later Sections, is via the spin ladder operators ($S^\pm = S^x \pm iS^y$), which have the properties that

$$\begin{aligned} S^+ |\uparrow\rangle &= 0, & S^+ |\downarrow\rangle &= |\uparrow\rangle \\ S^- |\uparrow\rangle &= |\downarrow\rangle, & S^- |\downarrow\rangle &= 0 \end{aligned} \quad (1.5)$$

The Hamiltonian then becomes

$$H = J \sum_i^N \left[\frac{1}{2} (S_i^+ S_{i+1}^- + S_i^- S_{i+1}^+) \right] + J^z \sum_i^N (S_i^z S_{i+1}^z) \quad (1.6)$$

We will use this form implicitly while dealing with the Bethe Ansatz and explicitly when we deal with the Jordan-Wigner transformation.

By looking at the symmetries of the system we can reduce the effective size of the Hamiltonian. Consider the operator

$$S^z = \sum_i^N S_i^z \quad (1.7)$$

which measures the total number of up or down spins. Since it commutes with the Hamiltonian, we can restrict the subsets of a fixed number of spins up or down. As we extend this to all spin operators and define

$$\vec{S} = \sum_i^N \vec{S}_i \quad (1.8)$$

we see that this also commutes with the Hamiltonian. Since the spin operators form an SU(2) algebra, the spin chain also has SU(2) as a symmetry algebra, meaning that it is symmetric under global rotations of the unit sphere in which the spins exist. This also implies that the eigenstates of the Hamiltonian will arrange themselves in multiplets with respect to the algebra of SU(2).

1.1 || Relation to the Ising Model

Both the Heisenberg and Ising models constitute simplified models of magnetism in materials and magnetic phase transitions. Nevertheless, the models differ in their symmetric properties, which are crucial for determining certain universal¹ characteristics of phase transitions.

In the Ising model, we have spins S_i that can either take the value -1 or $+1$ with each spin living on each site of an arbitrary N-lattice. Typically, the interaction of spins is between nearest neighbors, with the Hamiltonian being

$$H_{Ising} = -J \sum_{i=1}^N S_i S_{i+1} \quad (1.9)$$

¹We will briefly touch on the subject of universality classes later in this section.

where we have specifically assumed a 1d model for simplicity.² If $J < 0$, it's energetically preferable for neighboring spins to point in the same direction, macroscopically meaning a ferromagnet, while if $J > 0$ the preference is to point to opposite directions, meaning an antiferromagnet.

The Heisenberg model looks extremely similar, except for the fact that spin now represents a three-dimensional unit vector (\vec{S}_i) pointing anywhere on the unit sphere. The Hamiltonian is therefore

$$H_{\text{Heisenberg}} = -J \sum_{i=1}^N \vec{S}_i \vec{S}_{i+1} \quad (1.10)$$

A Brief Discussion on Universality Classes

Although universality classes in general fall outside of the scope of this thesis, it is useful to know why symmetry properties are important.

As we approach the critical point of a continuous phase transition, the correlation length typically diverges. The longer and longer length scales then become relevant to understand the underlying physics of the system. If we imagine coarse graining the original spin system iteratively, the remaining spins represent the average behaviour of larger and larger patches of bare spins. If we repeat this process up to correlation length, we have generated a series of energy functions in terms of the spins, where each member of the series is related to a different length scale.

Even though the interactions between the average spins most probably includes different forms than those between the original spins, they are nevertheless constrained to the forms allowed by the symmetries of the original system. Thus, systems with same symmetry properties, follow a similar pattern during this so called coarse graining process.³ They will, therefore, share some universal features, with a specific example being that of the critical exponents, that describe how properties diverge (or go to zero) near the phase transition points. For a more detailed analysis of a critical exponent, that of the vanishing of magnetization approaching the critical temperature from the ordered phase, see Appendix B

Ising and Heisenberg Universality Classes

Focusing on particular dimensionality and lattice structures, in the Ising model the Hamiltonian of a specific configuration of spins is invariant under flipping every spin of the system ($+1 \rightarrow -1$ and vice versa). In the Heisenberg model, the Hamiltonian is invariant to applying the same rotation around the unit sphere to every spin in the system. Therefore the Ising model is symmetrical under global reflections of the spins, which is a discrete symmetry, whilst the Heisenberg model is symmetrical under rotations, which is a continuous symmetry.

²Also for consistency of notation with the rest of the thesis.

³Another way to phrase this is they they will "flow" into the same space of energy functions.

The Ising model is therefore useful for studying magnetic phase transitions in systems that exhibit its kind of symmetry, and if we're working in n spacial dimensions, the phase transitions in these systems belong to the n -dimensional Ising universality class. Systems with the symmetries of the Heisenberg model respectively belong to the n -dimensional Heisenberg universality class.

Also worth mentioning is the fact that if the third coordinate of the unit vectors of spins in the Heisenberg model is zero ($\vec{S}_i = [S_i^x, S_i^y, S_i^z = 0], \forall i \leq N$), the so called XY model, the spin becomes a unit vector that can point anywhere on the unit circle and the system lies somewhere in between the Ising and Heisenberg models. It contains a continuous symmetry under global rotations along the unit circle and phase transitions of systems with this kind of symmetry belong to the n -dimensional XY universality class.

1.2 || Relation to the Free Fermion Model

Jordan and Wigner[1] observed, in 1928, that the up and down states of a single spin can be seen as an occupied or empty fermion state, enabling them to make the mapping

$$|\uparrow\rangle = f^\dagger |0\rangle, \quad |\downarrow\rangle = |0\rangle \quad (1.11)$$

allowing an explicit representation of the spin ladder operators

$$\begin{aligned} S^+ &= f^\dagger = \begin{bmatrix} 0 & 1 \\ 0 & 0 \end{bmatrix} \\ S^- &= f = \begin{bmatrix} 0 & 0 \\ 1 & 0 \end{bmatrix} \end{aligned} \quad (1.12)$$

while the z component of the spin operator is written as

$$S^z = \frac{1}{2} [|\uparrow\rangle\langle\uparrow| - |\downarrow\rangle\langle\downarrow|] = f^\dagger f - \frac{1}{2} \quad (1.13)$$

The x and y components are given by

$$\begin{aligned} S^x &= \frac{1}{2}(f^\dagger + f) \\ S^y &= \frac{1}{2i}(f^\dagger - f) \end{aligned} \quad (1.14)$$

If there are more than one spin particles, the representation needs to be modified, due to the fact that while independent spin operators commute, independent fermions anticommute. We can overcome this difficulty by attaching a phase factor, called a string, to the fermions, so that in the Jordan-Wigner representation, the spin operator at site j is

$$S_j^+ = f_j^\dagger e^{i\phi_j} \quad (1.15)$$

where the phase operator ϕ_j contains the sum of all fermion occupancies at sites left of j

$$\phi_j = \pi \sum_{l < j} n_l \quad (1.16)$$

The operator $e^{i\phi_j}$ is thus known as a string operator.

Therefore, the complete transformation is

$$\begin{aligned} S_j^+ &= f_j^\dagger e^{i\pi \sum_{l < j} n_l} \\ S_j^- &= f_j e^{-i\pi \sum_{l < j} n_l} \\ S_j^z &= f_j^\dagger f_j - \frac{1}{2} \end{aligned} \quad (1.17)$$

In layman's terms we took a spin and transformed it into a fermion interacting with a string

$$\text{spin} \leftrightarrow \text{fermion} \times \text{string}$$

If we now look at the Heisenberg Hamiltonian in the spin ladder operators form

$$H = J \sum_i^N \left[\frac{1}{2} (S_i^+ S_{i+1}^- + S_i^- S_{i+1}^+) \right] + J^z \sum_i^N (S_i^z S_{i+1}^z) \quad (1.18)$$

the way to produce the fermionic form is to notice that, in the first term, all terms in the string operators cancel except for $e^{i\pi n_j}$, which doesn't effect the Hamiltonian and is therefore ignored. The first part of the first term becomes

$$\frac{J}{2} \sum_i^N S_i^+ S_{i+1}^- = \frac{J}{2} \sum_j f_j^\dagger f_{j+1} \quad (1.19)$$

and the second, being the Hermitian conjugate of the first, becomes

$$\frac{J}{2} \sum_i^N S_i^- S_{i+1}^+ = \frac{J}{2} \sum_j f_j f_{j+1}^\dagger \quad (1.20)$$

We see that this term, being the transverse component of the interaction, includes a hopping term in the fermionized Hamiltonian. Of note is the fact that should the spin interaction include next-nearest neighbours, the string terms would make a comeback.

The z component of the Hamiltonian becomes

$$J^z \sum_i^N (S_i^z S_{i+1}^z) = J^z \sum_j \left(n_{j+1} - \frac{1}{2} \right) \left(n_j - \frac{1}{2} \right) \quad (1.21)$$

So that the complete transformed Hamiltonian is

$$H = -\frac{J}{2} \sum_j (f_j^\dagger f_{j+1} + f_j f_{j+1}^\dagger) + J^z \sum_j n_j - J^z \sum_j n_j n_{j+1} \quad (1.22)$$

There are two important things to note. The first one is that the ferromagnetic interactions mean that the spin fermions are actually attracted to one another. The second one is that the XY model ($J^z = 0$) has no interaction term, so this can be mapped to a free fermion model. The latter was first shown by Lieb et al[2] who used this equivalence to study the physical properties of the XY model.

2 | Ferromagnetic Ground and Excited States

Let us consider the ferromagnetic Heisenberg Hamiltonian with nearest-neighbour interaction

$$H = J \sum_i^N \vec{S}_i \vec{S}_{i+1}, \text{ where } J < 0 \quad (2.1)$$

The total energy of the system is given by the sum of the bond energies E_i

$$\begin{aligned} E_i = J \vec{S}_i \vec{S}_{i+1} &= \frac{J}{2} \left[(\vec{S}_i + \vec{S}_{i+1})^2 - \vec{S}_i^2 - \vec{S}_{i+1}^2 \right] \\ &= |J|S(S+1) - \frac{|J|}{2}(\vec{S}_i + \vec{S}_{i+1})^2 \end{aligned} \quad (2.2)$$

which is minimised by taking the two spins parallel $|\vec{S}_i + \vec{S}_{i+1}| = 2S$ which gives us

$$(E_i)_{min} = |J|[S(S+1) - S(2S+1)] = -|J|S^2 \quad (2.3)$$

therefore the ground energy of the whole system is

$$E_{tot} = \sum_i^N (E_i)_{min} = -\frac{1}{2}N|J|S^2 \quad (2.4)$$

The thing to note is that the ground state is not unique. This is because to get the ground state we took all the spins parallel to minimise the bond energy $S_{tot} = NS$. However, since the Hamiltonian is rotationally invariant, turning the total spin into another direction does not change the energy and therefore the ground state must be $(2NS + 1)$ -fold degenerate.

This creates an issue. The partition function is defined as

$$\mathcal{Z} = \sum_j e^{-\beta E_j} \quad (2.5)$$

If we try to include all of the ground states in the partition function, statistical averaging would give zero expectation value for the total magnetization of a ferromagnet, since we would average over all possible orientations of the total spin. For a macroscopically large system, we can restrict the Hilbert space by choosing only one ground state and then consider the finite excitations above that ground state.

Let us consider two states $|\psi_1\rangle, |\psi_2\rangle$. Let $|\psi_1\rangle$ be polarised in the z-direction and $|\psi_2\rangle$ polarised in an angle ϑ with the z-axis. If we assume that a finite excitation above $|\psi_1\rangle$ is $n \ll N$ spins flipped over while $N - n$ spins remain polarised in the z-direction, then the product of this state with $|\psi_2\rangle$ approaches 0 as $N \rightarrow \infty$. In the same vein, as $N \rightarrow \infty$, every excitation above $|\psi_1\rangle$ is orthogonal to every excitation above $|\psi_2\rangle$, meaning that not only are ground states orthogonal in the thermodynamic limit, but the Hilbert spaces that we build from them as well. All states built from $|\psi_1\rangle$ have spin density $\langle S^z \rangle_1 = S$, whilst those of $|\psi_2\rangle$ have $\langle S^z \rangle_2 = S \cos(\vartheta)$. This implies that the excitations above one of those states is distinguishable from the other. It is therefore possible to properly define the partition function so that it includes only the states built from one of the ground states.

2.1 || Excited States via the Bethe Ansatz

The Bethe ansatz is an exact method for the calculations of the eigenvalues and eigenvectors of a select class of quantum many-body systems. It was presented in 1931 by Hans Bethe[3] to obtain the exact eigenvalues and eigenvectors of the one-dimensional spin- $\frac{1}{2}$ Heisenberg model, which, as we have already seen, is a linear array of electrons with uniform exchange interaction between nearest neighbours. Although nowadays many other quantum many-body systems are known to be solvable by a variant of the Bethe ansatz, we will present the original work, already notoriously complicated, solving the 1D ferromagnetic spin- $\frac{1}{2}$ Heisenberg model, with a modern approach.

The idea behind the Bethe ansatz is to consider the chosen ground state, which is an eigenstate of the Hamiltonian, with all the spins up and then flipping some spins.

We choose the ground state to be

$$|0\rangle = |\uparrow\uparrow\uparrow \dots \uparrow\rangle \quad (2.6)$$

with ground energy

$$H|0\rangle = E_0 = -\frac{JN}{4} \quad (2.7)$$

The next step is to flip a spin, which can be done using the spin ladder operators (S^\pm). A state with M flipped spins is written as

$$|n_1, \dots, n_M\rangle = S_{n_1}^- \dots S_M^- |0\rangle \quad (2.8)$$

So the eigenstate is of the form

$$|\psi\rangle = \sum_{1 \leq n_1 \leq \dots \leq n_M \leq N} a(n_1, \dots, n_M) |n_1, \dots, n_M\rangle \quad (2.9)$$

where $a(n_1, \dots, n_M)$ represent unknown coefficients. Because of the periodicity of the lattice, $a(n_1 + N, \dots, n_M) = a(n_1, \dots, n_M)$, the Bethe ansatz proposes that the form of those coefficients is

$$a(n_1, \dots, n_M) = \sum_{\sigma \in S_M} A_\sigma e^{ip_{\sigma_i} n_i} \quad (2.10)$$

which is a plain-wave ansatz. Each such flip¹ creates excitations that behave like quasi-particles called magnons, equivalently known and as quantized spin waves in the wave picture of quantum mechanics.

2.2 || A Single Magnon

Here we will only discuss the case for a single magnon, cases with more magnons are extensively discussed in [4, 6, 5]

¹Up to degeneration.

If we flip a single spin, there are N different states possible. If we call the lattice site with the flipped spin n , then the state will be

$$|n\rangle := S_n^- |0\rangle = |\dots \downarrow_n \dots\rangle \quad (2.11)$$

and the Hamiltonian acting on it will give us

$$H |n\rangle = -J \left(\frac{1}{2} |n-1\rangle + \frac{1}{2} |n+1\rangle + |n\rangle \right) \quad (2.12)$$

We can see here that the flipped spin behaves like some sort of quasi-particle, being able to travel around sites or stay put.

If we now want to study this new quasi-particle the most natural way to start is to write down the eigenvector of the momentum p

$$|p\rangle = \sum_n e^{ipn} |n\rangle \quad (2.13)$$

which is the discrete version of a plane-wave that we got by taking $a(n) = e^{ipn}$.

If we now go back and look at the Hamiltonian action on a flipped spin at some position n , we can see that it has a contribution from its neighbouring sites

$$H |p\rangle = \dots - \frac{J}{2} [e^{ip(n+1)} + e^{ip(n-1)} - e^{ipn}] |n\rangle \dots \quad (2.14)$$

Therefore we see that $|p\rangle$ is an eigenstate of the Hamiltonian, with corresponding energy

$$E = 2J \sin^2 \left(\frac{p}{2} \right) \quad (2.15)$$

so the magnon is a quasi-particle with momentum p and energy E moving in the ground state.

As we impose periodicity, it acts as a quantization condition on the momentum which can be seen by acting with the Hamiltonian on the N th site. Since we get a contribution from n_1 instead of n_{N+1} , we find that this is an eigenstate with eigenvalue E

$$e^{ipN} = 1 \quad (2.16)$$

which is the momentum quantization condition for a particle on a circle of length N .

3 | Real-Space Renormalisation Group

The idea behind RG processes came when, in 1966, Leo Kadanoff[7] proposed that spins can be transformed into superspins, shaped from blocks of spins, for Ising-like models and proving some empirical¹ relations.

Phase transitions had mostly been studied in classical systems, where the Ising model has been solved exactly in two dimensions[8] and the Kondo problem was famously solved by Wilson in 1975[9]. If we want to study the low temperature behaviour of physical systems, we have to take into account the quantum nature of such systems, since it affects phase transition phenomena.

This is because the universality ideas that have emerged lead to the fact that the critical behaviour should be affected by quantum effects at low temperatures, which implies that the existence of quantum transitions at $T = 0$ creates quantum-classical crossover phenomena in classical low temperature transitions. Because of this, real-space renormalisation group methods have been expanded to quantum systems at $T \neq 0$, whilst at $T = 0$ the block renormalisation group method has been introduced to study the ground state and the excited states of many-body quantum systems, allowing for the study of transitions which take place in the ground state of the system.

In 1977, H.P. van der Braak et al[10], used the Block RG method to study the AF Heisenberg model while some years later, in 1979, Dasgupta, Ma and Hu[11, 12], developed their own real space RG process to study the low-temperature properties of the random AF Heisenberg model in 1D.

3.1 || RSRG of the AF Heisenberg Model

As shown already, the isotropic antiferromagnetic Hamiltonian is

$$H = J \sum_{i=1}^N S_i^x S_{i+1}^x + S_i^y S_{i+1}^y + S_i^z S_{i+1}^z \quad (3.1)$$

If we want to study the more general anisotropic model, for purposes what will become apparent later, it's useful to assume that $J^x = J^y = 1$ and $J^z = \gamma$, $0 \leq \gamma \leq 1$, so that the Hamiltonian takes the form

$$H = \sum_{i=1}^N S_i^x S_{i+1}^x + S_i^y S_{i+1}^y + \gamma S_i^z S_{i+1}^z \quad (3.2)$$

We may now group lattice sites into groups of three, labelling the pairs as (k, a) with $k = 1, 2, \dots, 1/3N$ specifying the block and $a = 1, 2, 3$ specifying the sites within each block, thus the n th lattice site is labelled as (k, a) where $n = 3k - 3 + a$. Since the lattice sites are in

¹Empirical at the time.

groups of three, the block will have half-integer spin which retains the properties of the original degrees of freedom. The Hamiltonian is then decomposed into two separate pieces, H_{in} and H_{out} , where H_{in} is the Hamiltonian of the couples inside a group and H_{out} the Hamiltonian coupling sites in adjacent blocks.

$$\begin{aligned}
H_{in} &= \sum_k \left[S^x(k, 1)S^x(k, 2) + S^x(k, 2)S^x(k, 3) \right. \\
&\quad + S^y(k, 1)S^y(k, 2) + S^y(k, 2)S^y(k, 3) \\
&\quad \left. + \gamma(S^z(k, 1)S^z(k, 2) + S^z(k, 2)S^z(k, 3)) \right] \\
H_{out} &= \sum_k \left[S^x(k, 3)S^x(k+1, 1) + S^y(k, 3)S^y(k+1, 1) \right. \\
&\quad \left. + \gamma(S^z(k, 3)S^z(k+1, 1)) \right]
\end{aligned} \tag{3.3}$$

The next step is to diagonalise H_{in} which can be achieved by considering a single block

$$\begin{aligned}
H_{in} &= \sum_k H_{block}(k) \\
H_{block} &= \vec{S}(1)\vec{S}(2) + \vec{S}(2)\vec{S}(3) + \epsilon(S^z(1)S^z(2) + S^z(2)S^z(3)) \\
&= \frac{1}{2} \left[(\vec{S}(1) + \vec{S}(2) + \vec{S}(3))^2 - (\vec{S}(1) + \vec{S}(3))^2 - \frac{3}{2} \right] \\
&\quad + \epsilon(S^z(1)S^z(2) + S^z(2)S^z(3))
\end{aligned} \tag{3.4}$$

where $\epsilon = \gamma - 1$.

For $\epsilon = 0$, the isotropic case, H_{block} is rotationally invariant, and the eigenstates can be found by combining $\vec{S}(1)$ and $\vec{S}(3)$ to get a total spin of 0 or 1, which is then coupled to $\vec{S}(2)$ giving us a spin- $\frac{3}{2}$ multiplet and two spin- $\frac{1}{2}$ doublets

$$\begin{aligned}
\left| \frac{3}{2}, \frac{3}{2} \right\rangle &= |\uparrow\uparrow\uparrow\rangle, \quad E = +\frac{1}{2} \\
\left| \frac{3}{2}, \frac{1}{2} \right\rangle &= \frac{1}{\sqrt{3}} (|\downarrow\uparrow\uparrow\rangle + |\uparrow\downarrow\uparrow\rangle + |\uparrow\uparrow\downarrow\rangle), \quad E = +\frac{1}{2} \\
\left| \frac{1}{2}, \frac{1}{2} \right\rangle_1 &= \frac{1}{\sqrt{6}} (|\downarrow\uparrow\uparrow\rangle + 2|\uparrow\downarrow\uparrow\rangle + |\uparrow\uparrow\downarrow\rangle), \quad E = -1 \\
\left| \frac{1}{2}, \frac{1}{2} \right\rangle_0 &= \frac{1}{\sqrt{2}} (|\uparrow\uparrow\downarrow\rangle - |\downarrow\uparrow\uparrow\rangle), \quad E = 0
\end{aligned} \tag{3.5}$$

plus the four corresponding to all the spins flipped with negative total S .

For $\epsilon \neq 0$, H_{block} has the discrete symmetry $z \rightarrow -z$ and is also invariant only under rotations about the z -axis. This means that the states of different total spin but equal S^z can coexist. The state $\left| \frac{3}{2}, \frac{3}{2} \right\rangle$ is still an eigenstate, with energy $E = \frac{1}{2}\gamma$, as is the state $\left| \frac{1}{2}, \frac{1}{2} \right\rangle_0$, with

energy $E = 0$, but the states $|\frac{1}{2}, \frac{1}{2}\rangle_1$ and $|\frac{3}{2}, \frac{1}{2}\rangle$ mix with each other. If we diagonalize the 2×2 matrix, we get the lowest energy eigenstate

$$\begin{aligned} \left|+\frac{1}{2}\right\rangle &= \frac{1}{1+2x^2} \left(\left|\frac{1}{2}, \frac{1}{2}\right\rangle_1 + \sqrt{2x} \left|\frac{3}{2}, \frac{1}{2}\right\rangle \right) \\ E &= -\frac{1}{4} [\gamma + (\gamma^2 + 8)^{1/2}] \\ x &:= \frac{2(\gamma - 1)}{8 + \gamma + 3(\gamma^2 + 8)} \end{aligned} \quad (3.6)$$

Since the eigenvalues form a complete set, we could get an equivalent description by specifying the eigenstate of each block. A good argument to help us is that the low-lying states of the lattice are predominantly formed by the low lying eigenstates of H_{block} , which allows us to restrict our attention to the sector of states built exclusively from the block states $|+\frac{1}{2}\rangle$ and $|-\frac{1}{2}\rangle$, where $|-\frac{1}{2}\rangle$ is given from $|+\frac{1}{2}\rangle$ under $z \rightarrow -z$.

$$\begin{aligned} \left|+\frac{1}{2}\right\rangle &= \frac{1}{\sqrt{1+2x^2}} \frac{1}{\sqrt{6}} \left[(2x-1) |\downarrow\uparrow\uparrow\rangle + (2x+2) |\uparrow\downarrow\uparrow\rangle + (2x-1) |\uparrow\uparrow\downarrow\rangle \right] \\ \left|-\frac{1}{2}\right\rangle &= -\frac{1}{\sqrt{1+2x^2}} \frac{1}{\sqrt{6}} \left[(2x-1) |\uparrow\downarrow\downarrow\rangle + (2x+2) |\downarrow\uparrow\downarrow\rangle + (2x-1) |\downarrow\downarrow\uparrow\rangle \right] \end{aligned} \quad (3.7)$$

The next step is to form an effective Hamiltonian, whose matrix elements are the same as the original in this state sector.

Construction of the Effective Hamiltonian

The effective Hamiltonian is constructed by defining new spin operators \vec{S}' such that

$$\begin{aligned} \left\langle \frac{1}{2}, +\frac{1}{2} \left| \vec{S}'_z \right| \frac{1}{2}, +\frac{1}{2} \right\rangle_1 &= +\frac{1}{2} \\ \left\langle \frac{1}{2}, -\frac{1}{2} \left| \vec{S}'_z \right| \frac{1}{2}, -\frac{1}{2} \right\rangle_1 &= -\frac{1}{2} \\ &\vdots \end{aligned} \quad (3.8)$$

Using this definition we can easily calculate that in each block

$$\begin{aligned} \langle S^x(1) \rangle &= \langle S^x(3) \rangle = \frac{2(1+x)(1-2x)}{3(1+2x^2)} \langle S^{x'} \rangle \\ \langle S^y(1) \rangle &= \langle S^y(3) \rangle = \frac{2(1+x)(1-2x)}{3(1+2x^2)} \langle S^{y'} \rangle \\ \langle S^z(1) \rangle &= \langle S^z(3) \rangle = \frac{2(1+x)^2}{3(1+2x^2)} \langle S^{z'} \rangle \end{aligned} \quad (3.9)$$

where the $\langle S^i \rangle$ implies any one of the four matrix elements involving the states $|\pm\frac{1}{2}\rangle$ and the equality $\langle S^i(1) \rangle = \langle S^i(3) \rangle$ is due to the even parity of the states. From the above, we can

eliminate the \vec{S} operators from H_{out} and since H_{in} has already been diagonalised we can form the effective Hamiltonian

$$H^{(1)} = \sum_{i=1}^{N/3} a_1 + \sum_{i=1}^{N/3-1} b_1 [S^{x'}(k)S^{x'}(k+1) + S^{y'}(k)S^{y'}(k+1) + \gamma_1 S^{z'}(k)S^{z'}(k+1)] \quad (3.10)$$

where a_1, b_1 are given by

$$\begin{aligned} a_1 &= -\frac{1}{4}[\gamma + \sqrt{\gamma^2 + 8}] \\ b_1 &= \left(\frac{2(1+x)(1-2x)}{3(1+2x^2)} \right)^2 \\ \gamma_1 &= \left(\frac{1+x}{1-2x} \right)^2 \gamma \end{aligned} \quad (3.11)$$

Since the form of the effective Hamiltonian is essentially the same as that of the original Hamiltonian, apart from the energy shift a_1 and the scaling factor b_1 , the blocks can be seen as the sites of a new lattice where we can follow an identical procedure on $H^{(1)}$ to get $H^{(2)}$, etc.

In this way we can repeat the procedure m times giving us a sequence of Hamiltonians $H^{(m)}$ increasing the length scale each time and following the recursion relations

$$H^{(m)} = \sum_{k=1}^{N/3^m} a_m + \sum_{k=1}^{(N/3^m)-1} b_m [S_x(k)S_x(k+1) + S_y(k)S_y(k+1) + \gamma_m S_z(k)S_z(k+1)] \quad (3.12)$$

$$\begin{aligned} a_{m+1} &= 3a_m - \frac{1}{4}b_m [\gamma_m + (\gamma_m^2 + 8)^{1/2}] \\ b_{m+1} &= b_m \left(\frac{2(1+x_m)(1-2x_m)}{3(1+2x_m^2)} \right)^2 \\ \gamma_{m+1} &= \gamma_m \left(\frac{1+x_m}{1-2x_m} \right)^2 \\ a_0 &= 0, \quad b_0 = 1, \quad \gamma_0 = \gamma \end{aligned}$$

where

$$x_m \equiv 2(\gamma_m - 1) \left[8 + \gamma_m + 3(\gamma_m^2 + 8)^{1/2} \right]^{-1}$$

In this context, a_m shows the contribution to the energy, which becomes the dominant contribution after sufficiently many iterations of the BRG process. On the finite lattice of length N , the number of iterations needed is approximately $m = \log_3 N$ [13], so that after m iterations

the whole lattice has been reduced to a single block, meaning that a_m is the sole contributor to the energy. Since every iteration reduces the lattice sites by a factor $\frac{1}{3}$, the energy per original lattice site is computed as $a_m/3^m \equiv \mathcal{E}_m$. If we let $N \rightarrow \infty$, we get the infinite lattice, which yields an energy density given by

$$\mathcal{E}_{m+1} = \mathcal{E}_m - \frac{1}{12(3^m)} b_m [\gamma_m + (\gamma_m^2 + 8)^{\frac{1}{2}}], \text{ where } \mathcal{E}_0 = 0 \quad (3.13)$$

Due to the nature of the RG process, the set of states in each step is smaller than the previous one, meaning that the above equation can always be seen as an upper bound of the true energy density.

Fixed Points

The recursion relations (3.12) have three fixed points in the region $\gamma \geq 0$. Here we will only discuss the fixed point $\gamma = 0$, which is the XY model, the other two being $\gamma = 1$ and $\gamma \rightarrow \infty$ [13].

Near $\gamma = 0$, the RG equations reduce to

$$\begin{aligned} \gamma_{m+1} &= \frac{1}{2} \gamma_m \\ b_{m+1} &= \left[\frac{1}{2} + \mathcal{O}(\gamma_m) \right] b_m \\ \mathcal{E}_{m+1} &= \mathcal{E}_m - \frac{1}{12(3^m)} b_m (2\sqrt{2} + \gamma_m) \end{aligned} \quad (3.14)$$

The first recursion relation of (3.14) implies that if $|\gamma|$ is small, the system flows towards the XY form, so that the $\gamma = 0$ fixed point is stable. The second relation implies that $\lim_{m \rightarrow \infty} b_m = 0$, so that the XY model is a massless theory. This means that after sufficiently many iterations we can construct states with an arbitrarily small excitation energy.

Finally, calculating the energy density \mathcal{E}_m at the point $\gamma = 0$ using (3.14) gives us

$$\mathcal{E}_{m+1} = \mathcal{E}_m - \frac{\sqrt{2}}{6^{m+1}} \quad (3.15)$$

which, for $m \rightarrow \infty$ gives us a geometric series, whose sum is

$$\mathcal{E}_\infty = -\frac{\sqrt{2}}{5} = -0.2828 \quad (3.16)$$

which, when compared with the exact result [2] yields an error of 11%.

4 | SDRG Method for the Random AF Model

Renormalization methods in pure systems usually involve a finite number of coupling constants, in contrast with renormalization methods in disordered systems, which involve probability distributions that live in an infinite dimensional space. This increases the difficulty of the study of the RG flow, since now we study complex functionals instead of critical exponents and the fixed points are much harder to find. This extra difficulty usually leads to the necessity of numerical solutions or to additional approximations consisting of projections into finite spaces by choosing certain analytical forms for distributions with a limited number of parameters. There is a small number of RG flows that are simple enough to be analyzed completely, whose fixed point distributions usually have interesting probabilistic interpretations, the Dasgupta-Ma RG method being one of them.

The Dasgupta-Ma RG method, as introduced by Dasgupta and Ma[12], has two important properties. The first one is that the renormalization concerns the extreme value of a random variable, which determines the scale and evolves via the renormalization, and serves as the cut-off point of the renormalized distribution. The second property is that the renormalization is local in space, meaning that in each step only the immediate neighbours of the aforementioned random variable are concerned by the RG procedure.

4.1 || Dasgupta-Ma RG Method for the Heisenberg Model

Most generally, the Heisenberg model with random couplings and anisotropy is

$$H = \sum_i^N \vec{J}_i \vec{S}_i \vec{S}_{i+1} \quad (4.1)$$

The coupling constants J_i show quenched randomness, meaning they are randomly distributed in space, but fixed in time, following a certain distribution function $P(J)$, $0 < J < \max J = \Omega$. Because of this, the chain does not have translational invariance which causes the system to not have a spin-wave spectrum. It is therefore easier (if not the only possible way) to find approximate solutions for the problem of arbitrary $P(J)$.

If we want to decimate a general random XYZ chain, we have to pick the bond with the largest of the possible J . Without loss of generality, we name that bond the $n = 2$ bond, so the local Hamiltonian takes the form

$$\mathcal{H}_{23} = \vec{J}_2 \vec{S}_2 \vec{S}_3 \quad (4.2)$$

Because the bond 2 – 3 is the strongest, we are able to handle the bonds 1 – 4 perturbatively, which is shown in Appendix B. This means that the 1 – 4 Hamiltonian is of the form

$$\mathcal{H}_{14} = E'_{14} + \vec{J}'_{14} \vec{S}'_1 \vec{S}'_4 \quad (4.3)$$

where

$$J_{1-4}^x = \frac{J_1^x J_3^x}{J_2^y + J_2^z} \quad (4.4)$$

the approximated perturbation of the bond in the x direction¹. By ignoring the stable term², and by taking the $\vec{J}_{1,3} \ll \vec{J}_2$, we get that $\tilde{S}_{1,4} = S_{1,4}$ up to $\mathcal{O}(J_{1,3}/J_2)$ [14] and therefore the effective Hamiltonian in (3.3) will yield the correct ground energy, low-energy spectrum, and low-temperature correlation functions of S_1 and S_4 . We shall use the recursion relation (4.4) as the basis for the renormalisation group transformations for the rest of the chapter.

The flow equation takes the form of

$$\frac{\partial P}{\partial J} = R[P] \quad (4.5)$$

where $R[P]$ is a complex functional.

4.2 || RG Flow Equation for the XX Chain

For the rest of the discussion we shall only consider the simplest case, that of the XX chain with $J^x = J^y = J$. The recursion relation then becomes

$$J^z = 0, \quad \tilde{J} = \frac{J_1 J_3}{J_2} \quad (4.6)$$

and defining the strongest bond is simply $\Omega := \max(J)$.

Because of the new recursion relation, it is convenient to transform our variables to logarithmic, defining

$$\begin{aligned} \Gamma &:= -\ln(\Omega) \\ \zeta &:= \ln(\Omega/J) \end{aligned} \quad (4.7)$$

where obviously $\zeta \geq 0$ and large $\zeta \rightarrow$ small J .

Again the recursion relation changes. This time (4.6) becomes

$$\zeta = \zeta_1 + \zeta_3 - \zeta_\Omega = \zeta_1 + \zeta_3 = \zeta_- + \zeta_+ \quad (4.8)$$

Having defined these new logarithmic variables, we can express the distribution of bonds as $P(\zeta, \Gamma)$, with the probability of a bond ζ at a fixed scale Γ being $P(\zeta, \Gamma)d\zeta = dP(\zeta, \Gamma)$. With every step of the elimination transformation, Γ changes to $\Gamma + \delta\Gamma$, firstly because of the change of $\zeta \rightarrow \zeta'$

$$\zeta' = \ln\left(\frac{\Omega'}{J}\right) = \ln\left(\frac{\Omega}{J}\right) - \Gamma + \Gamma' = \zeta + \delta\Gamma \quad (4.9)$$

and secondly from the fact that in the elimination process, a new bond is added, namely \tilde{J} .

¹Likewise for $J_{1-4}^{y,z}$.

²The stable term would be useful to calculate things such as the ground energy, but in general can be emitted.

Combining those two contributions, near the limit where $\delta\Gamma \rightarrow 0$, the distribution $P(\zeta, \Gamma)d\zeta$ of bonds ζ at scale Γ becomes

$$\frac{\partial}{\partial\Gamma}P(\zeta, \Gamma) = \frac{\partial}{\partial\zeta}P(\zeta, \Gamma) + P(0, \Gamma) \int_0^\infty d\zeta_- \int_0^\infty d\zeta_+ \delta(\zeta - \zeta_+ - \zeta_-) P(\zeta_+, \Gamma) P(\zeta_-, \Gamma) \quad (4.10)$$

where $P(0, \Gamma)d\Gamma$ is the fraction of bonds with ζ in the range 0 to $d\Gamma$. Since ζ_- , ζ_+ represent the bonds on each side (left and right respectively), the recursion relation makes an appearance inside the delta function of the integral, which ensures that for each ζ , we are adding the corresponding probability of obtaining an effective bond with that value to the new distribution.

4.3 || Fixed Points and the Random Singlet Phase

If we look for fixed point solutions for the RG flow (3.10), a natural approach is to rescale ζ to an appropriate power of Γ , κ , since in this model the randomness always leads to a critical point.

By defining

$$\eta = \frac{\zeta}{\Gamma^\kappa} \quad (4.11)$$

the distribution transforms to

$$P(\zeta, \Gamma) = \frac{1}{\Gamma^\kappa} Q(\eta, \Gamma) \quad (4.12)$$

and therefore the flow equation becomes

$$\Gamma \frac{\partial Q}{\partial\Gamma} = \kappa \left(Q + \eta \frac{\partial Q}{\partial\eta} \right) + \Gamma^{1-\kappa} \left(\frac{\partial Q}{\partial\eta} + Q(0, \Gamma) \int_0^\eta d\eta' Q(\eta', \Gamma) Q(\eta - \eta', \Gamma) \right) \quad (4.13)$$

For $\kappa > 1$ the second term vanishes, leaving the fixed point equation as

$$\frac{\partial Q}{\partial\eta} = -\frac{Q}{\eta} \quad (4.14)$$

giving the trivial solution of $Q(\eta) = C/\eta$, which diverges for small η , i.e. approaching the strongest bond.

For $\kappa < 1$ the second term dominates, leaving the fixed point equation as

$$\frac{\partial Q}{\partial\eta} = -Q(0) \int_0^\eta d\eta' Q(\eta') Q(\eta - \eta') \quad (4.15)$$

who's solution, using Laplace transformations, can be shown to oscillate in sign for big η . [15].

Both the aforementioned solutions are unphysical when it comes to the behaviour of fixed points, thus the only physical solution left is $\kappa = 1$ as a possible scale exponent, leaving us only with

$$\Gamma \frac{\partial Q}{\partial\Gamma} = Q(\eta, \Gamma) + (1 + \eta) \frac{\partial Q}{\partial\eta} + Q(0, \Gamma) \int_0^\eta d\eta' Q(\eta', \Gamma) Q(\eta - \eta', \Gamma) \quad (4.16)$$

Looking for solutions of $Q^*(\eta)$, independent of Γ , and therefore $\frac{\partial Q}{\partial \Gamma} = 0$, we get the fixed point equation, which has a one-parameter family of solutions, parametrized by $Q_0^* = Q^*(0)$.

By Laplace transforming $Q \rightarrow \hat{Q}$,

$$z \frac{\partial \hat{Q}}{\partial z} = z \hat{Q} + Q_0 [\hat{Q}^2 - 1] \quad (4.17)$$

where Q_0 is constrained by

$$Q_0 = Q(0) = \lim_{\eta \rightarrow 0^+} \frac{i}{2\pi i} \int_{c-i\infty}^{c+i\infty} dz \hat{Q}(z) e^{z\eta} \quad (4.18)$$

and by linearizing \hat{Q} via the transformation

$$\hat{Q} = \frac{-z}{u Q_0} \frac{du}{dz} \quad (4.19)$$

equation (3.15) becomes

$$\frac{d^2 u}{dz^2} + \left(\frac{1}{z} - 1 \right) \frac{du}{dz} - \frac{Q_0^2}{z^2} u = 0 \quad (4.20)$$

Using the Frobenius method[15] we find that $Q_0 = Q(0)$ parametrizes a family of solutions to the above equation, which when plugged into (3.14) gives the Laplace transformation of the distribution. Using the inverse Laplace transform is then the fixed points we were looking for.

To narrow down the possible fixed point solutions, we must distinguish between whether or not Q_0 is an integer. If $2Q_0$ is not an integer, instead of using the Frobenius method, we can use the simpler

$$u = \sum_{n=0}^{\infty} u_n z^n \quad (4.21)$$

where u_n is given by the recursion relation

$$u_{n+1} = \frac{n - Q_0}{(n+1)(n+1-2Q_0)} u_n \quad (4.22)$$

implying that for large positive z , $u(z) \sim z^a e^z$ so that $\hat{Q} \approx -z/Q_0$ which is unphysical[14]. Therefore $2Q_0 = m$ is an integer, which implies a $z^m \ln z$ part in u [14] forcing a $1/\eta^{2Q_0+1}$ tail in $Q(\eta)$. The only exception is if $m = 2$, meaning $Q(0) = 1$, where in this case $u = 1 + z$.

In the case where $Q_0 = 1$, the general form of \hat{Q} is explicitly given by

$$\hat{Q} = \frac{1 + C' e^z (1 - z)}{1 + z + C' e^z} \quad (4.23)$$

where the only value of C' that gives the proper large z behaviour $\hat{Q} \approx Q_0/z$, corresponding to the discontinuity at $\eta = 0$ is $C' = 0$.

This means that the only fixed point that behaves well is

$$\hat{Q} = \frac{1}{1+z} \quad (4.24)$$

yielding

$$Q^*(\eta) = e^{-\eta} \Theta(\eta) \quad (4.25)$$

where $\Theta(\eta)$ is the Heaviside step function. This is the random singlet fixed point distribution, which can be shown to be stable under perturbations exponentially decaying in η . [14]

If we want to express this distribution in terms of the original spin chain distribution, remembering that $\kappa = 1$

$$P^*(\zeta, \Gamma) = \frac{1}{\Gamma} e^{-\zeta/\Gamma} \Theta(\zeta) \quad (4.26)$$

and by reverting back from the logarithmic parameters to our original bonds,

$$P^*(J, \Omega) = \frac{\alpha}{\Omega} \left(\frac{\Omega}{J} \right)^{1-\alpha} \Theta(\Omega - J) \quad (4.27)$$

where

$$\alpha = 1/\Gamma = -1/\ln \Omega \quad (4.28)$$

If we remember the RG process, during each step we paired the two spins with strongest bond in a singlet, replacing them with an effective bond between the neighbouring spins. Repeating this process enough times, the total effective bond between two spins at along distance can become the strongest bond in the chain, causing the two spins to be paired in a long ranged singlet.

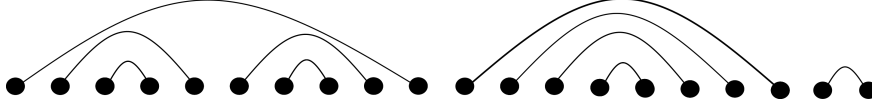


Figure 4.1: A schematic of the random singlet phase. Pairs of spins, connected via bonds form singlets over arbitrarily long distances. Notice that bonds do not overlap.

At low energies, the system consists mostly of pairs of spins coupled together into singlets over arbitrarily long distances, shown in Figure 3.1. This critical point, described by the distribution (3.23) is known as the random singlet phase.

4.4 || Physical Properties

Since the ground state of the random spin chain is composed by singlet pairs, where the spins can be arbitrarily remote and the effective interaction between them is rapidly decreasing with the distance, in order to assess the strength of the long bonds we must determine the relation between the energy and length scales. The probability of connected spins at scale Γ

is $P(0, \Gamma)$, so when Γ is increased by $d\Gamma$, a fraction $2P(0, \Gamma)d\Gamma$ of the spins left are removed. Near the fixed point, $P(0, \Gamma) = Q(0, \Gamma)/\Gamma \approx Q_0^*/\Gamma = 1/\Gamma$, the number of spins n changes due to the renormalisation step

$$\frac{dn}{d\Gamma} = -2 \frac{Q_0^*}{\Gamma} n_\Gamma = \frac{-2}{\Gamma} n_\Gamma \quad (4.29)$$

meaning that the fraction of non-decimated spins at the new energy scale is

$$n_\Gamma = \frac{1}{\Gamma^2} \quad (4.30)$$

The typical length between the remaining spins at energy scale Γ is therefore

$$L(\Gamma) \sim \frac{1}{n_\Gamma} \sim \Gamma^2 \sim [\ln(\Omega)]^2 \quad (4.31)$$

which makes sense, since each $\ln J$ is a sum, with alternating signs of a series of $\ln J_n$. If there was no correlation between the remaining spins at scale Γ and the bonds appearing in the sum, then the sum would be an asymptotically Gaussian random variable, having mean zero and variance such that $\Gamma \sim \sqrt{L}$. The form of (4.31) is that of a dynamical scaling at an infinite disorder fixed point.

Low Temperature Susceptibility

The low temperature susceptibility is estimated by studying how the system is affected when exposed to external fields for different ratios of thermal energy T and energy scale Ω . In the low temperature case, $\Omega \gg T$, the strongly coupled pairs are very weakly excited by the fluctuations of the thermal energy, whilst in the opposite limit, $T \gg \Omega$, the remaining pairs are very weakly coupled, since $J \ll T$, and they are therefore uncoupled and free to contribute to the Curie susceptibility, which goes as $\sim T$. In this case, one should stop the renormalization procedure at the limit where $\Omega = T$, where the remaining spins, that have a density $n_\Gamma \sim \ln^2(\Omega/T)$, all contribute by a Curie susceptibility giving

$$\chi \sim \chi_z \sim \frac{n_{\Gamma_T}}{T} \sim \frac{1}{T [\ln \frac{\Omega}{T}]^2} \quad (4.32)$$

The transverse and longitudinal susceptibilities have the same singular behaviour where the Curie-type susceptibility is modified by log-type corrections. Because these corrections are very strong, they typically lead in measuring effective temperature dependent critical exponents.

Average Pair Correlation Function

The average pair correlation function between two spins at distance $r \sim L$ is dominated by the remaining spins at length scale L , because the decimated spins form singlets, the correlation between spins of different singlets is negligible. The probability to have a free spin at length scale L is $n_{\Gamma_L} \sim 1/L$, whilst for 2 spins it's $n_{\Gamma_L}^2$. There's a finite probability that under further

decimation, the two spins will form a singlet, and will therefore have a correlation $C(r) = \mathcal{O}(1)$. If we average the correlation over spin-pairs with mutual distance r , we get

$$\langle C(r) \rangle \sim \frac{(-1)^r}{r^2} \quad (4.33)$$

By considering two randomly chosen spins at distance r , we expect that typically they will belong to different singlet pairs, and therefore the typical correlations will be very weak. If the length scale during the decimation is $L = r$, the two spins become nearest neighbours with effective coupling $J_L \sim \Omega_L$ which measures the size of these correlations. We therefore have

$$-\ln C_{typ}(r) \sim \ln \Omega_L \sim \Gamma_L^{-1} \sim \frac{1}{L^{1/2}} \sim \frac{1}{r^{1/2}} \quad (4.34)$$

which is completely different from the average correlation function. We therefore note that the correlation function in the random singlet phase is non-self averaging.

5 | Numerical Dasgupta-Ma RG

5.1 || Introduction to the Model

In order to better grasp the ideas presented in the previous chapter, and also to appreciate the complexity of the Strong Disorder RG, we created a numerical model to simulate the process using Python.

If we wanted to simulate the nearest-neighbour spin chain we would need two rows, one for each left spin and one for each right spin.

$$\begin{aligned}\text{left spin} &:= [1 \ 2 \ 3 \ 4 \ \dots \ N - 1] \\ \text{right spin} &:= [2 \ 3 \ 4 \ 5 \ \dots \ N]\end{aligned}$$

where the bonds would then form a matrix

		Right spin					
		2	3	4	5	...	N
L e f t s p i n	1	J_1					
	2		J_2				
	3			J_3			
	4				J_4		
	\vdots					\ddots	
	$N - 1$						J_{N-1}

which, after an iteration of the RG method would look like

		Right spin					
		2	3	4	5	...	N
L e f t s p i n	1	J_1					
	2		0		\tilde{J}_{24}		
	3			singlet			
	4				0		
	\vdots					\ddots	
	$N - 1$						J_{N-1}

so that the two spins interacting with the new effective bond being between spins $[2, 5]$, since the spins $[3, 4]$ form a singlet. This means that we can effectively represent a spin chain using only a bond matrix, so that the column represents the left spin and the row the right spin, i.e. a bond in the $[i, j]$ position of the matrix would denote an interaction between \vec{S}_i and \vec{S}_{j+1} .

The first step then, is to make an $N \times N$ matrix with the diagonal taking random values using the uniform distribution

$$P(J) = \begin{cases} \frac{1}{b-a}, & x \in [b, a] \\ 0, & \text{everywhere else} \end{cases} \quad (5.1)$$

where without loss of generality, we can set $a = 0$, $b = 1$. This means that all the values of the strength of the bonds will range between 0 and 1 (Fig.5.1).

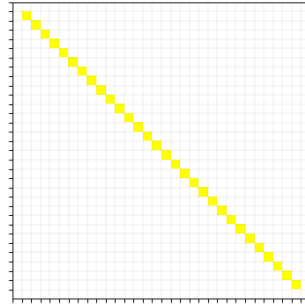


Figure 5.1: This is the matrix for a spin chain with 30 spin particles. Note that the top left and bottom right positions are empty. This is due to the fact that we simulated an aperiodic, finite chain.

We then follow the process as explained by Dasgupta, Ma and Hu[11, 12], finding the strongest bond, decimating it and replacing it with a new effective bond (Fig 5.2). In order to avoid the singlet bond randomly been picked for the elimination transformation, we give it a negative value.

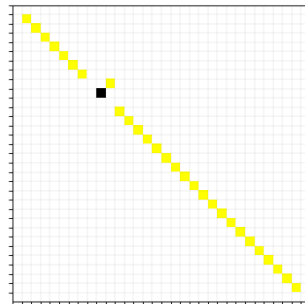


Figure 5.2: The new matrix generated after a single iteration of the RG method. The black colour indicates a singlet, which is "trapped" under the new effective bond as expected.

By continuing the iterations we end up with even more singlets, and the possibility of long-range interacting spins is made visible (Fig. 5.3).

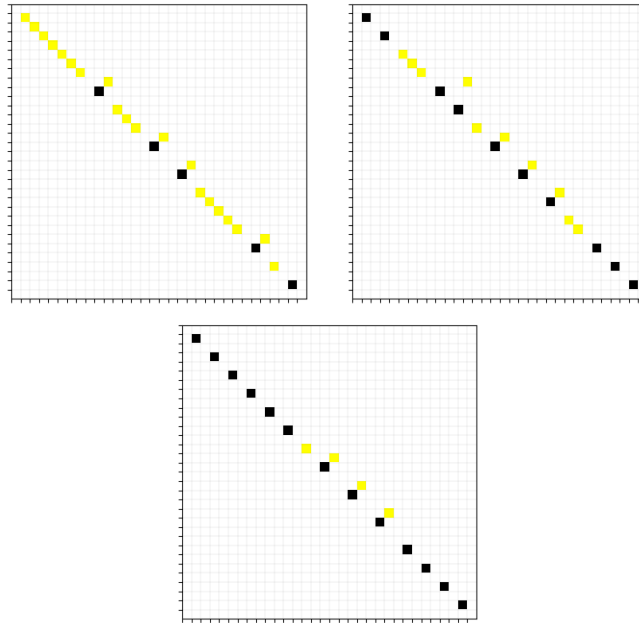


Figure 5.3: Different stages of the RG process. As more bonds are decimated we get a glimpse of the long range bonds between spins comprising a singlet, represented by the deviation from the main diagonal.

As the final iteration resolves, we reach the random singlet state, comprising of singlets formed over arbitrary distances (Fig. 5.4).

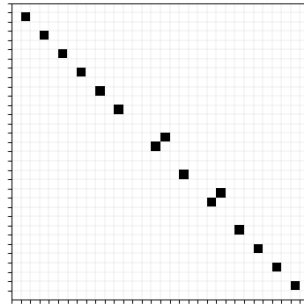


Figure 5.4: The random singlet phase, where all bonds of the spin chain have been replaced by singlets. As we can see, we end up with singlets that are connected over arbitrarily long distances.

To make the figures eligible, we chose to have a small number of starting bonds, meaning that only a very small number of singlets will have formed with non-initial nearest neighbours. Should we scale this up, we would get both more long singlets as well as longer singlets.

5.2 || Results

Unfortunately, due to the aperiodic nature of the system, it is impossible to define ζ for every step of the iteration, due to the fact that sometimes, the strongest bond will be the one on either edge of the chain. The way to circumvent this problem is to assume that if the strongest bond Ω is in an edge location, rather than $J_{\pm} = 0$, J_{\pm} takes an infinitesimal value $\varepsilon > 0$ so that $J_{\pm} \ll \Omega \Rightarrow \zeta \ll 1$ and therefore we can assume $\eta = 0$.

To see the fixed point distribution (Eq.4.25) we sort all the non-zero values of η during the RG process and for each step summing over the values to the right, essentially approximating a CDF (Fig. 5.5).

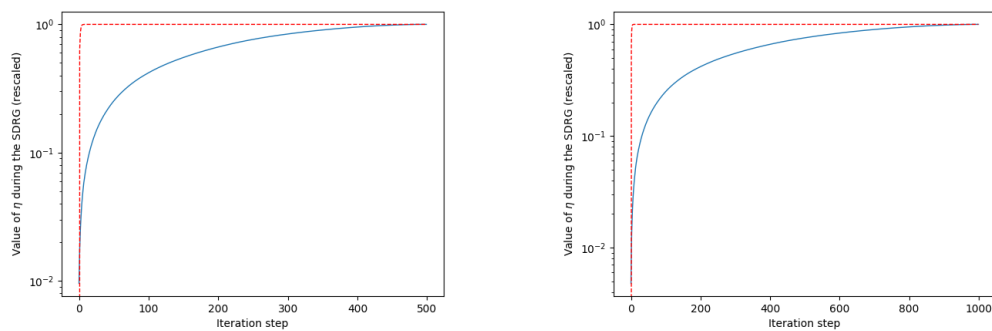


Figure 5.5: Two different CDFs of η for different lengths of the spin chain. The right one has $N = 1001$ spins, while the left one has $N = 2001$. The red dotted line is the CDF of the exponential distribution over the range of the iteration steps.

If we zoom in on the area near the end of the process, we see that as we near the random singlet phase, the exponential CDF indeed acts as a stable fixed point for the CDF of η (Fig. 5.6).

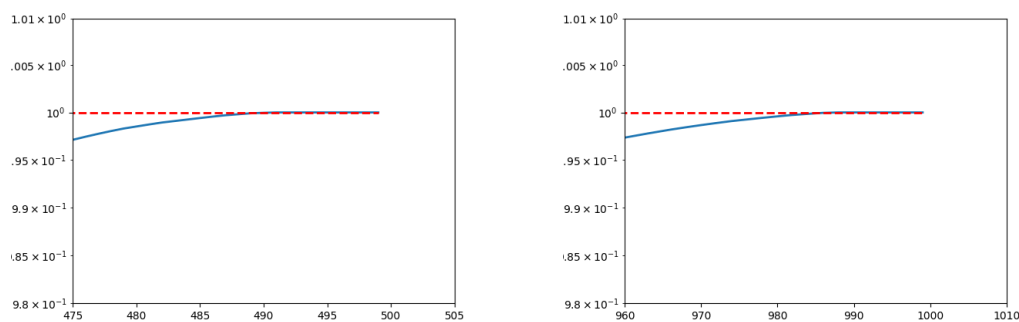


Figure 5.6: Here we can see how the CDF of η approaches the fixed point Q^* for the aforementioned systems.

As we can see from (Fig. 5.5), as we increase the number of spins N , the CDF of η during the RG goes to the CDF of the exponential distribution. An expected behaviour would be that, as we approach $N \rightarrow \infty$, we would see the CDF of η become asymptotically exactly the CDF of the exponential distribution.

Last but not least, the length between spins during the RG process is shown (Fig. 5.7).

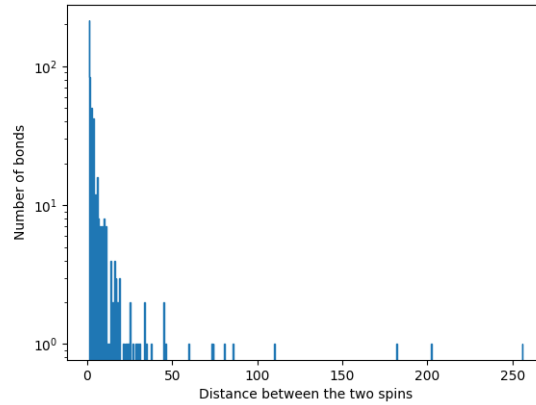


Figure 5.7: The number of bonds sharing the same distance on a system with 1001 spins. We can see how a very small number of spins share a bond over very long distances.

Appendices

A | The Heisenberg Hamiltonian

When we take a look at a system of two electrons the Hamiltonian is

$$H\Phi = H_0\Phi + V\Phi = E\Phi \quad (\text{A.1})$$

where Φ is the spatial wavefunction, V the Coulomb interaction between the two electrons and H_0 is the basic Hamiltonian

$$H_0 = \frac{p^2}{2m} \quad (\text{A.2})$$

By including the spin interaction, the state of the combination of the electrons is in a superposition of the states

$$\Psi = \begin{cases} \Phi_s |s\rangle \\ \Phi_t |t\rangle \end{cases} \quad (\text{A.3})$$

where $|s\rangle$ is the singlet and $|t\rangle$ is the triplet state.

Since we're dealing with fermions, due to the Pauli exclusion principle, the wavefunction Ψ must be anti-symmetric and therefore Φ_s must be symmetric, whilst Φ_t is anti-symmetric.

Because of the different symmetric properties, the expected value of the Coulomb energy is different for the singlet state and the triplet state. The difference, symbolised as J is

$$J := E_s - E_t = \langle \Phi_s | V | \Phi_s \rangle - \langle \Phi_t | V | \Phi_t \rangle \quad (\text{A.4})$$

J is also known as the *exchange integral*. We can see why if, once we express $\Phi_{s/t}$ as

$$\Phi_{s/t} := \Phi_{\pm} = \frac{1}{\sqrt{2}} [\phi_a(r_1)\phi_b(r_2) \pm \phi_a(r_2)\phi_b(r_1)] \quad (\text{A.5})$$

and remember what Dirac notation is, we write

$$J = 2 \iint dr_1 dr_2 \phi_a^*(r_1)\phi_b^*(r_2)V\phi_a(r_2)\phi_b(r_1) \quad (\text{A.6})$$

The symmetry of the spins decides the symmetry of the spatial wavefunctions meaning that the alignment of the spins determines the electrostatic energy $\langle \Psi | V | \Psi \rangle$. In the singlet state the spins are antiparallel while, in the triplet state, they are parallel. Because J is derived solely from a spin-independent Hamiltonian, it serves as an indication for the dependance of the Coulomb energy from the orientation of the spins.

The sign of J carries a special significance. If J is positive, the system is said to be ferromagnetic, while if it's negative, the system is said to be antiferromagnetic. Because the spatial states are sufficient to study the electromagnetic properties, for each pair of electrons we have four states. We can combine the singlet and triplet states by defining a new Hamiltonian

$$H_{1,2} = \left(\frac{1}{4}E_s + \frac{3}{4}E_t \right) - (E_s - E_t)\vec{S}_1\vec{S}_2 \quad (\text{A.7})$$

By ignoring the constant term, since it's only contribution is to shift the ground state energy, we can rewrite the new Hamiltonian as

$$H_{1,2} = -J\vec{S}_1\vec{S}_2 \quad (\text{A.8})$$

The above is the Heisenberg Hamiltonian for a pair of electrons. If we want to expand to a solid with N electrons, we should probably account for the effect of the lattice on the states and how that affects the interactions between the electrons, but we don't. Instead, we expand the Hamiltonian by assuming that each electron simply interacts with every other in the same way and we sum over all interactions. The effects of the lattice are then assumed to act as an external field on each spin

$$H = -\sum_{ij} J_{ij}\vec{S}_i\vec{S}_j - g\mu_B H \sum_i \vec{S}_i \quad (\text{A.9})$$

By ignoring the external field and assuming that the interaction is weaker as we move further from each spin and keep only the terms with nearest neighbour interactions, we can simplify even further. In this case, the Hamiltonian changes again to take the form

$$H = -J \sum_i \vec{S}_i\vec{S}_{i+1} \quad (\text{A.10})$$

B | Perturbation of the Random XX Spin Chain

The local Hamiltonian, considering solely the bond between the spins \vec{S}_2 and \vec{S}_3 is

$$H_0 = J_2 \vec{S}_2 \cdot \vec{S}_3 \quad (\text{B.1})$$

This XX system has a singlet state as its ground state $|s\rangle$ and three triplet states as the excited states $|t\rangle$. In the basis of S^z

$$|s\rangle = \frac{1}{\sqrt{2}}(|\uparrow\downarrow\rangle - |\downarrow\uparrow\rangle) \quad (\text{B.2})$$

$$|t_1\rangle = |\uparrow\uparrow\rangle \quad (\text{B.3})$$

$$|t_0\rangle = \frac{1}{\sqrt{2}}(|\uparrow\downarrow\rangle + |\downarrow\uparrow\rangle) \quad (\text{B.4})$$

$$|t_{-1}\rangle = |\downarrow\downarrow\rangle \quad (\text{B.5})$$

If we use the spin ladder operations, we can rewrite the Hamiltonian as

$$H_0 = \frac{J_2}{2} (S_1^+ S_2^- + S_1^- S_2^+) \quad (\text{B.6})$$

from which we get

$$\begin{aligned} E_s &= -\frac{1}{2} J_2 \\ E_{t_1} &= E_{t_{-1}} = 0 \\ E_{t_0} &= \frac{1}{2} J_2 \end{aligned} \quad (\text{B.7})$$

If we add the contributions of the nearest neighbours, \vec{S}_1 , \vec{S}_4 , and by the assumption that J_2 is the strongest bond, we can treat J_1 , J_3 perturbatively, giving us the Hamiltonian

$$H = H_0 + \mathcal{H} \quad (\text{B.8})$$

where \mathcal{H} is given by

$$\mathcal{H} = J_1 \vec{S}_1 \cdot \vec{S}_2 + J_3 \vec{S}_3 \cdot \vec{S}_4 \quad (\text{B.9})$$

Perturbatively expanding around \mathcal{H} , modifies the energy of the ground state E_s by

$$E_s \rightarrow E_s + \langle s | \mathcal{H} | s \rangle + \sum_t |\langle s | \mathcal{H} | t \rangle|^2 \frac{1}{E_s - E_t} \quad (\text{B.10})$$

Using Eq.(B.6), for fixed \vec{S}_1 , \vec{S}_4 , we can show that

$$\begin{aligned} \langle s | \mathcal{H} | s \rangle &= \langle s | \mathcal{H} | t_0 \rangle = 0 \\ |\langle s | \mathcal{H} | t_1 \rangle|^2 &= \frac{1}{8} [J_1^2 \vec{S}_1^+ \vec{S}_1^- + J_3^2 \vec{S}_4^+ \vec{S}_4^- - J_1 J_3 (\vec{S}_1^+ \vec{S}_4^- + \vec{S}_4^+ \vec{S}_1^-)] \\ |\langle s | \mathcal{H} | t_{-1} \rangle|^2 &= \frac{1}{8} [J_1^2 \vec{S}_1^- \vec{S}_1^+ + J_3^2 \vec{S}_4^- \vec{S}_4^+ - J_1 J_3 (\vec{S}_1^- \vec{S}_4^+ + \vec{S}_4^- \vec{S}_1^+)] \end{aligned} \quad (\text{B.11})$$

Thus, the sum becomes

$$\sum_t |\langle s | \mathcal{H} | t \rangle|^2 \frac{1}{E_s - E_t} = -\frac{2}{J_2} \left[\frac{J_1^2}{8} (\vec{S}_1^+ \vec{S}_1^- + \vec{S}_1^- \vec{S}_1^+) + \frac{J_3^2}{8} (\vec{S}_4^+ \vec{S}_4^- + \vec{S}_4^- \vec{S}_4^+) \right. \\ \left. - \frac{J_1 J_3}{4} (\vec{S}_1^+ \vec{S}_4^- + \vec{S}_4^+ \vec{S}_1^-) \right] \quad (\text{B.12})$$

The sums of the form $\vec{S}_i^+ \vec{S}_i^- + \vec{S}_i^- \vec{S}_i^+$ act on the same spin and exhibit a very useful behaviour. S^+ annihilates an up spin, whilst S^- annihilates a down spin. This means that whenever this duet of operators in the parenthesis act upon a state, one of them becomes 0, while the other one leaves the state unchanged. This means that the previous cumbersome equality simplifies to

$$\sum_t |\langle s | \mathcal{H} | t \rangle|^2 \frac{1}{E_s - E_t} = -\frac{2}{J_2} \left[\frac{J_1^2}{8} + \frac{J_3^2}{8} - \frac{J_1 J_3}{4} (\vec{S}_1 \cdot \vec{S}_4) \right] \quad (\text{B.13})$$

where we inverted back from Eq.(B.6).

Rearranging and plugging the results into the perturbation introduced earlier in this Appendix, we end up with

$$E_s = E'_s + J' \vec{S}_1 \cdot \vec{S}_4 \quad (\text{B.14})$$

where

$$E'_s = -\frac{1}{2} J_2 - \frac{1}{4 J_2} (J_1^2 + J_3^2) \\ J' = \frac{J_1 J_3}{J_2} \quad (\text{B.15})$$

Bibliography

- [1] P. Jordan and E. Wigner. “Über das Paulische Äquivalenzverbot.” In: *Zeitschrift für Physik* 47.9 (1928), pp. 631–651. doi: 10.1007/BF01331938.
- [2] Elliott Lieb, Theodore Schultz, and Daniel Mattis. “Two soluble models of an antiferromagnetic chain.” In: *Annals of Physics* 16.3 (1961), pp. 407–466. doi: 10.1016/0003-4916(61)90115-4.
- [3] H. Bethe. “Zur Theorie der Metalle.” In: *Zeitschrift für Physik* 71.3 (1931), pp. 205–226. doi: 10.1007/BF01341708.
- [4] Patrick Fazekas. *Lecture Notes on Electron Correlation and Magnetism*. Vol. 5. Series in Modern Condensed Matter Physics. WORLD SCIENTIFIC, 1999.
- [5] N.W.M. Plantz. “The Coordinate BetheAnsatz for the Heisenberg XXX model.” Seminar Notes. Seminar Notes. Jan. 22, 2018. URL: <http://andreghenriques.com/Seminars/SpinChainsTalk1.pdf>.
- [6] Marius de Leeuw and Constantin Candu. “magnon1.” Seminar Notes. Seminar Notes. ETH Zurich, Institute for Theoretical Physics, 2013. URL: <https://edu.itp.phys.ethz.ch/fs13/int/SpinChains.pdf>.
- [7] Leo P. Kadanoff. “Scaling laws for ising models near T_c .” In: *Physics Physique Fizika* 2.6 (1966), pp. 263–272. doi: 10.1103/PhysicsPhysiqueFizika.2.263.
- [8] Lars Onsager. “Crystal Statistics. I. A Two-Dimensional Model with an Order-Disorder Transition.” In: *Physical Review* 65.3 (Feb. 1, 1944), pp. 117–149. doi: 10.1103/PhysRev.65.117.
- [9] Kenneth G. Wilson. “The renormalization group: Critical phenomena and the Kondo problem.” In: *Reviews of Modern Physics* 47.4 (1975), pp. 773–840. doi: 10.1103/RevModPhys.47.773.
- [10] H. P. Van de Braak et al. “The determination of the ground-state energy of an antiferromagnetic lattice by means of a renormalization procedure.” In: *Physica A: Statistical Mechanics and its Applications* 87.2 (1977), pp. 354–368. doi: [https://doi.org/10.1016/0378-4371\(77\)90022-X](https://doi.org/10.1016/0378-4371(77)90022-X).
- [11] Shang-keng Ma, Chandan Dasgupta, and Chin-kun Hu. “Random Antiferromagnetic Chain.” In: *Physical Review Letters* 43.19 (1979), pp. 1434–1437. doi: 10.1103/PhysRevLett.43.1434.
- [12] Chandan Dasgupta and Shang-keng Ma. “Low-temperature properties of the random Heisenberg antiferromagnetic chain.” In: *Physical Review B* 22.3 (1980), pp. 1305–1319. doi: 10.1103/PhysRevB.22.1305.
- [13] Jeffrey M. Rabin. “Renormalization-group studies of antiferromagnetic chains. I. Nearest-neighbor interactions.” In: *Physical Review B* 21.5 (Mar. 1, 1980), pp. 2027–2037. doi: 10.1103/PhysRevB.21.2027.
- [14] Daniel S. Fisher. “Random antiferromagnetic quantum spin chains.” In: *Physical Review B* 50.6 (1994), pp. 3799–3821. doi: 10.1103/PhysRevB.50.3799.

- [15] Mauricio Fonseca Fernández. “Dasgupta-Ma Renormalization in the Random Heisenberg XX model and the Random Singlet Phase.” In: (2018). URL: https://jscaux.org/static/jsc/courses/2017-18_StudSem/MINI_DIGESTS/Random_Singlet_Phase-Mauricio_Fonseca-11834218.pdf.
- [16] Javier Rodriguez-Laguna. “Real Space Renormalization Group Techniques and Applications.” PhD thesis. Complutense University of Madrid, 2002. 161 pp. URL: <https://arxiv.org/abs/cond-mat/0207340>.
- [17] V. E. Korepin, N. M. Bogoliubov, and A. G. Izergin. *Quantum Inverse Scattering Method and Correlation Functions*. Cambridge Monographs on Mathematical Physics. Cambridge University Press, 1993. ISBN: 978-0-521-58646-7. DOI: 10.1017/CBO9780511628832.
- [18] Piers Coleman. *Introduction to Many-Body Physics*. Cambridge University Press, 2015. ISBN: 978-1-139-02091-6. DOI: 10.1017/CBO9781139020916.
- [19] Leo P. Kadanoff. “Variational Principles and Approximate Renormalization Group Calculations.” In: *Phys. Rev. Lett.* 34.16 (1975), pp. 1005–1008. DOI: 10.1103/PhysRevLett.34.1005.
- [20] Ferenc Igloi and Cécile Monthus. “Strong disorder RG approach of random systems.” In: *Physics Reports* 412.5 (2005), pp. 277–431. DOI: <https://doi.org/10.1016/j.physrep.2005.02.006>.
- [21] Fabio Franchini. “Notes on Bethe Ansatz Techniques.” In: (2011). URL: <https://people.sissa.it/~ffranchi/BAnotes.pdf>.
- [22] Subir Sachdev. *Quantum Phase Transitions*. 2nd ed. Cambridge: Cambridge University Press, 2011. ISBN: 978-0-521-51468-2. DOI: 10.1017/CBO9780511973765.
- [23] Theodre Burkhardt and J. M. J. van Leeuwen, eds. *Real-Space Renormalization*. Topics in Current Physics. Berlin Heidelberg: Springer-Verlag, 1982. ISBN: 978-3-642-81827-1. DOI: 10.1007/978-3-642-81825-7.
- [24] Bambi Hu. “Introduction to real-space renormalization-group methods in critical and chaotic phenomena.” In: *Physics Reports* 91.5 (Nov. 1, 1982), pp. 233–295. ISSN: 0370-1573. DOI: 10.1016/0370-1573(82)90057-6.